Probing spin susceptibility of a correlated two-dimensional electron system by transport and magnetization measurements

V. M. Pudalov,[1,2,*] A. Yu. Kuntsevich,[1] M. E. Gershenson,[3] I. S. Burmistrov,[4,5,6,7] and M. Reznikov[8]

[1]*P. N. Lebedev Physical Institute, 119991 Moscow, Russia*

[2]*National Research University Higher School of Economics, Moscow 101000, Russia*

[3]*Serin Physics Lab, Rutgers University, Piscataway, New Jersey 08854, USA*

[4]*L. D. Landau Institute for Theoretical Physics RAS, 119334 Moscow, Russia*

[5]*Laboratory for Condensed Matter Physics, National Research University Higher School of Economics, 101000 Moscow, Russia*

[6]*Institut für Theorie der Kondensierten Materie, Karlsruhe Institute of Technology, 76128 Karlsruhe, Germany*

[7]*Institut für Nanotechnologie, Karlsruhe Institute of Technology, 76021 Karlsruhe, Germany*

[8]*Solid State Institute, Technion, 3200003 Haifa, Israel*

(Received 2 January 2018; revised manuscript received 24 May 2018; published 3 October 2018)

We report temperature and density dependences of the spin susceptibility of strongly interacting electrons in Si inversion layers. We measured (i) the itinerant electron susceptibility χ^* from the Shubnikov-de Haas oscillations in crossed magnetic fields and (ii) thermodynamic susceptibility χ_T sensitive to all the electrons in the layer. Both χ^* and χ_T are strongly enhanced with lowering the electron density in the metallic phase. However, there is no sign of divergency of either quantity at the density of the metal-insulator transition n_c. Moreover, the value of χ_T, which can be measured across the transition down to very low densities deep in the insulating phase, increases with density at $n < n_c$, as expected. In the absence of magnetic field, we found the temperature dependence of χ^* to be consistent with Fermi-liquid-based predictions, and to be much weaker than the power law predicted by non-Fermi-liquid models. We attribute a much stronger temperature dependence of χ_T to localized spin droplets. In strong enough in-plane magnetic field, we found the temperature dependence of χ^* to be stronger than that expected for the Fermi liquid interaction corrections.

DOI: 10.1103/PhysRevB.98.155109

I. INTRODUCTION

Dilute two-dimensional electron systems (2DES) provide unique opportunity for exploring the physics of strongly interacting charged fermions, with spin properties of these systems being of particular interest.

Within the framework of the Landau theory of Fermi liquid (FL), interacting electrons are described as a system of quasiparticles with renormalized-by-interaction parameters, such as compressibility κ^*, effective mass m^*, spin susceptibility χ^*, and g-factor g^* [1–4]. These parameters are predicted to grow with lowering temperature and density, and their measurement is an important test of the theory. Strong renormalization of χ^* and m^* was indeed observed in ^{3}He and is well-explained within the framework of the FL theory [1,2].

Disorder, especially in 2DES, greatly complicates the problem, bringing into play another parameter, the density n_c of the apparent metal-insulator transition (MIT). This parameter happened to be very important: the spin susceptibility χ^* has been consistently found to grow strongly as the density n is lowered toward n_c. Increase of χ^* relative to the nonrenormalized Pauli susceptibility χ_P by a factor of 7 with decreasing electron density [5,6] was deduced from Shubnikov-de Haas (ShdH) oscillations in tilted or crossed magnetic fields [7–12] and from analysis of the in-plane magnetoresistance (MR) data [13–15].

Strong renormalization of χ^* with $n \to n_c$ raised an intriguing possibility of magnetic instability [16] of a diluted disordered 2DES. As a result, much effort was invested in extracting χ^* as a function of *density*, typically at the lowest accessible temperature, with several papers claiming divergent χ^* with $n \to n_c$ and $T \to 0$, and therefore a quantum phase transition. Temperature dependence of χ^*, which provides an important test for the theoretical models, was somehow overlooked.

In this paper, we focus on the temperature dependence of the spin susceptibility obtained from magneto-oscillatory transport (χ^*) and from thermodynamic (χ_T) measurements of high-mobility dilute electron gas in Si inversion layers. We, (i) on the basis of both χ^* and χ_T, refute the claim for magnetic instability at $n = n_c$, (ii) report temperature dependence of χ^*, which happened to be weak and not entirely consistent with available theories, and (iii) report thermodynamic susceptibility χ_T, which is large and strongly temperature-dependent. Finally, we discuss the reason for the discrepancy between χ^* and χ_T.

A. Density dependence of χ^*: A brief overview

In a clean system, ferromagnetic instability originates solely from the combined effect of electron-electron interactions and the Pauli principle. In metals, the long-range part of

*pudalov@lebedev.ru

the Coulomb interaction is screened, whereas the short-range part leads to strong correlations in the electron liquid. In clean metals, this short-range part of the interaction leads to ferromagnetic (Stoner) instability at sufficiently strong interaction. Critical r_s values for the expected instability in a single-valley 2D system varied from 13 to 20 in early calculations [5,6,17]. According to them, the ferromagnetic transition is likely to be of the first order with a complete, rather than partial spin polarization. More recent numerical Monte Carlo calculations [18–20] predicted a stable, fully polarized liquid phase at $T = 0$ for $r_s > 25-26$, before the Wigner crystallization occurs at around $r_s \approx 35 - 37$ [21]. The valley degree of freedom, even twofold, suppresses the tendency to spin polarization, making the fully spin-polarized state unstable [22,23].

Disorder, on the contrary, favors spin polarization. Within the Wigner-Mott model [24,25], the effective mass and thus the spin susceptibility are predicted to diverge in the vicinity of the MIT: $\chi \propto (n - n_c)^{-1}$, though, according to numerical calculation [26], the system stays unpolarized in the accessible density range ($r_s < 10$) at not-too-strong disorder ($1/k_F l \lesssim 1$).

In this context, a strong in-plane field-induced MR in Si inversion layers [27,28] was interpreted in Refs. [13–15] as a signature of ferromagnetic instability at, or very close to $n_c \approx 0.8 \times 10^{11}\,\mathrm{cm}^{-2}$ in the studied samples, corresponding to $r_s \approx 9$.

B. Theoretical studies of the temperature dependence of $\chi^*(T)$: A brief overview

Within the FL theory, Fukuyama [29] and Altshuler *et al.* [30] calculated interaction corrections to electron spin susceptibility for a 2DES system in the *diffusive regime* (low temperatures, $T\tau \ll 1$) to be

$$\frac{\Delta\chi^*(T)}{\chi_P} \sim -\frac{1}{k_F l}\ln(T\tau). \tag{1}$$

Here $\chi_P = 2\mu_B^2 m_b/\pi$ stands for nonrenormalized Pauli susceptibility of electrons with bulk effective mass m_b and twofold valley degeneracy, τ is the momentum relaxation time, k_F and l denote the Fermi momentum and the mean free path, respectively. Throughout the paper, we use units with $\hbar = k_B = e = 1$. Taking into account the valley multiplicity $n_v = 2$ for (100)-Si, and introducing the relevant FL parameters (see Appendix A), this formula can be written as

$$\frac{\chi^*(T) - \chi_P^*}{\chi_P^*} = \frac{\delta\chi^*(T)}{\chi_P^*} \approx \frac{2}{\pi k_F l}\frac{n_v F_0^\sigma}{\left(1 + F_0^\sigma\right)}\ln(T\tau), \tag{2}$$

where $\chi_P^* = n_v\mu_B^2 m^*/[\pi(1 + F_0^\sigma)]$ is the spin susceptibility of the FL at $T = 0$, which includes FL-type renormalization in the absence of disorder, m^* is the effective mass renormalized by the electron-electron interaction, and F_0^σ denotes the FL interaction parameter in the particle-hole triplet channel.

In the *ballistic regime* (high temperatures, $T\tau \gg 1$), the leading-order in T correction to $\chi^*(T)$ for the 2D FL was found to be proportional to the temperature [31–36]

$$\Delta\chi^*(T) = \chi_P^* A^2 \frac{T}{4E_F}, \tag{3}$$

where E_F is the Fermi energy. Within the theory of interaction quantum corrections for a single-valley system A is given in Ref. [35] by $A = (m^*/m_b)\sum_{n=0}^{\infty}(-1)^n(2n+1)F_n^\sigma/(1 + F_n^\sigma)$. Here m_b denotes the nonrenormalized band electron mass. The particular expression for A depends on the parameter range and the approximation used.

Within the interval $r_s = 3 - 7$ of our measurements, $|F_0^\sigma| \approx 0.3 \div 0.5$ is large [12,37], $n = 0$ term in the series of harmonics dominates, and Eq. (3) acquires a simple form [33,35]:

$$\frac{\Delta\chi^*(T)}{\chi_P^*} \approx \frac{T}{2E_F}G, \tag{4}$$

where $G \approx (m^*/m_b)/(1 + F_0^\sigma) \sim 1$ varies from 1.6 to 2.7 as r_s increases from 3 to 7. It was noted in Ref. [35] that prefactor A in Eq. (3) determines also the slope of the linear-in-T correction to the conductivity $\Delta\sigma(T)$ of the 2D FL in the ballistic regime [38–40]. The temperature dependence of the conductivity and magnetoconductivity was carefully studied in Refs. [37,41] and found to be consistent with the calculated interaction corrections [39]. This agreement encouraged us to perform comparison of $\Delta\chi^*(T)$ with the predictions based on the theory of interaction corrections.

We note that in the experimentally accessible parameter range, both ballistic and diffusive interaction corrections Eqs. (2)–(4) are expected to be rather small: $\Delta\chi^*/\chi_P^* \lesssim 3\%$. For high-mobility Si-MOSFETs, the accessible temperature range is set by $0.05 < T\tau < 5$; the upper bound is determined by the temperature $T^* \sim 10\,\mathrm{K}$, at which $\tau_\varphi(T^*)$ becomes comparable with τ and quantum coherence vanishes.

With temperature decrease, the system is anticipated to enter the diffusive regime, $T\tau \ll 1$. Within two-parameter renormalization group (RG) theory, interactions become renormalized by the dimensionless parameter $\ln(l_\phi/l) = -\ln(T\tau)$, where l_ϕ is the phase breaking length. Particularly, spin susceptibility is predicted to grow strongly as $T \to 0$ [42–44]: $\chi^* \propto T^{-\zeta}$ with $\zeta < 1$ [45].

An important question is whether a 2D system of itinerant electrons undergoes spin ordering and conventional FL model breaks down when the interactions are strong and $T \to 0$ [46,47]. In particular, Khodel *et al.* [47] predicted that the quasiparticle energy spectrum $\varepsilon(k)$ flattens at the Fermi level as a result of interactions, and, above a certain critical value $r_s \approx 7$, the 2D Fermi surface (a circle) breaks into the nested rings [47]. This dispersion instability should result in an essentially non-FL behavior, which would lead to strong temperature dependence of the spin susceptibility $\chi^* \propto T^{-2/3}$ [48,49].

The mean field theory [50] suggests that a low-dimensional disordered system may undergo a finite-temperature spin polarization at significantly weaker interaction strength than its clean counterpart. The theory predicts divergence of the spin susceptibility χ^* at a disorder-dependent temperature T_c, below which the system should become ferromagnetic. This tendency toward ferromagnetic transition originates from the effective enhancement of interactions by diffusive dynamics of electrons.

To summarize this brief overview, FL theory and numerical Monte-Carlo calculations predict only a weak temperature dependence of χ^* and no ferromagnetic instability for a

multivalley system. By contrast, a number of other theories [42–44,48–50] predict divergence of χ^* in the vicinity of metal insulator or topological transition in a 2D system.

C. Experimental studies of the density and temperature dependence of χ and their interpretation

On the experimental side, we are not aware of any *direct measurements* of the temperature dependence of χ^* for the itinerant 2D electrons by transport techniques such as magnetotransport and quantum magnetooscillations. Particularly, in ShdH oscillation measurements [8,9,51], no temperature dependence of the susceptibility was observed. Indeed, this dependence is very weak, as seen from our data, and therefore requires high-precision ShdH measurements in vector fields.

In Refs. [52,53], the temperature dependence of the weak field in-plane magnetoconductivity in the vicinity of n_c was found to behave as $\Delta\sigma \propto (B^2/T^2)T^{-\varepsilon}$; the factor $T^{-\varepsilon}$ was conjectured to originate from the renormalization of $\chi^*(T)$ in the spirit of the two-parameter RG theory [54]. Clearly, this interpretation is model dependent. Based on such interpretation, the strong growth of $\chi^*(T)$ was reported in Refs. [52,53,55]. Later, in Refs. [56,57], this MR behavior was attributed to semiclassical effects in the two-phase non-FL state. We also note that the magnetotransport measurements in tilted magnetic fields [58], performed with the same or similar Si-MOS samples as those in Refs. [52,53,55], revealed that the in-plane MR cannot be described by electron-electron interaction correction only. Simple evidence is that the observed strong parallel field MR quickly diminishes when the perpendicular field component is applied on top of the parallel field [58]. These inconsistencies question the assumption required for the applicability of the RG approach.

As the density decreases and interactions increase, a part of the itinerant electrons become localized already well above the critical density n_c [59]. This tendency strengthens with density approaching n_c. In contrast to the transport measurements, which are sensitive to the most conductive parts of a sample, thermodynamic measurements [59–61] probe the magnetization averaged over the *whole 2D system*. Since the localized and mobile electrons coexist and strongly interact, magnetic state of the localized electrons may affect the transport properties.

Strongly temperature-dependent $\partial M/\partial n \equiv -\partial\mu/\partial B$ was observed already in Ref. [60]. However, contrary to the predictions of the FL-theory in the ballistic regime [31,33–35] for the Pauli-type susceptibility, the measured thermodynamic paramagnetic susceptibility [60] *grew* as temperature decreased. To account for the anomalous sign of the $d\chi/dT$ found in Ref. [60], Shekhter and Finkel'stein considered rescattering of pairs in the Cooper channel, which leads to anomalous temperature dependence $\Delta(1/\chi(T)) \propto -T$ in the ballistic regime [62,63].

Reference [60] mostly discussed magnetization in strong magnetic fields, $\mu_B B/k_B T \gg 1$. In subsequent thermodynamic measurements [59] performed in weaker magnetic fields, the magnetization-per-electron $\partial M/\partial n$ was found to overshoot the Bohr magneton at a magnetic field of $\mu_B B/k_B T \approx 0.25$, and thermodynamic susceptibility was found to grow much faster, as $\Delta\chi(T) \propto 1/T^2$. The low field data was shown to originate mainly from the collective localized spins whose contribution greatly dominates over and masks the Pauli spin magnetization of the mobile electrons [59]. This interpretation was supported by the theory [64].

II. EXPERIMENTAL

Both transport and thermodynamic magnetization measurements were performed on (100) Si-MOS samples from two different wafers: "small" samples, 2.5×0.25 mm, with moderate peak mobility $\mu^{\rm peak} \approx 2.4\,{\rm m}^2/{\rm Vs}$, (Si3-10, Si6-14), and "large" ones, 5×0.8 mm with high mobility $\mu^{\rm peak} \approx (3.2-3.4)\,{\rm m}^2/{\rm Vs}$ at $T = 0.3$ K (Si-5, Si-15, Si-UW1, Si-UW2). All samples had the 190 ± 20 nm thick gate oxide thermally grown in dry oxygen, atop of which an Al film (gate) was deposited by thermal evaporation. For crossed-field transport measurements, we preferably used small-size samples to ensure homogeneity over the sample area of the perpendicular field generated by a small split-coil system [65]. For the thermodynamic magnetization measurements, we mainly used large-size samples to increase the signal.

The carrier densities referred to throughout the paper have been found from the ShdH oscillations and the Hall effect measurements (more details are given in Appendix B). The elastic scattering time τ shown in the figures was measured following the approach of Refs. [37,39,41]. First, the temperature dependence of the conductivity σ was measured at zero field and relatively high temperatures, where σ linearly depends on T. Then, the $\sigma(T)$-dependence was linearly extrapolated to $T = 0$ and τ was found from $\sigma(T = 0)$ using the Drude formula.

A. Spin susceptibility χ^* of itinerant electrons probed by quantum magnetooscillations

We determined χ^* from the period and phase of the beating patterns of the ShdH oscillations [8]. In the crossed-field (or vector-field) technique, the in-plane component of the magnetic field partially spin polarizes the electron system, whereas a weak perpendicular component probes the density of electrons in the split spin-subbands (for details, see Ref. [65]). The data was collected over the temperature range $T = 0.1 - 1$ K for electron densities $n = (0.77 - 10) \times 10^{11}\,{\rm cm}^{-2}$, corresponding to the dimensionless interaction strength $r_s = 9.5 - 2.6$, respectively [5,6]. An AC current 0.1–1 nA at frequency 13 Hz was supplied from a battery operated current source to reduce the electron overheating [66].

Figure 1 shows an example of the raw ρ_{xx} data versus perpendicular field $B_\perp$; weak localization in fields $B_\perp < 0.1$ T, smooth monotonic MR, and ShdH oscillations are visible for $B_\perp > 0.15$ T. The data in Fig. 1 was taken with in-plane field $B_\parallel = 2.5$ T over the range $T = 0.3 - 1$ K.

To extract the oscillatory component, we subtracted the second-order polynomial [8] from the raw data (such as in Fig. 1). When the amplitude of oscillations is small, the remaining oscillatory component $\Delta\rho_{xx}$ is well described by the conventional Lifshits-Kosevich (LK) formula [67–70]. Application of an in-plane magnetic field induces beating of the ShdH oscillations [8]; examples of beating patterns at high and low electron densities are shown in Figs. 2 and 3,

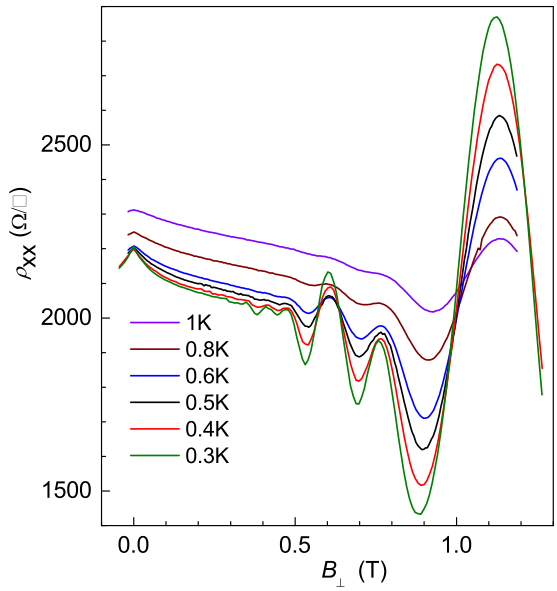

FIG. 1. Example of the $\rho_{xx}(B_\perp)$ data at different temperatures. $n \approx 2 \times 10^{11}$ cm^{-2} and $B_\parallel = 2.5$ T. "Large" high-μ sample.

respectively. For clarity, the $\delta\rho_{xx}(B_\perp)$ data was normalized by the amplitude $P_1(B_\perp)$ of the first harmonic of the oscillations [8,67,70] (for more details, see Appendix C).

One can see from Figs. 2 and 3 that the oscillations can be precisely fitted by the LK formula. Since $B_\parallel$ is weak relative to the polarizing field, and the interval of $B_\perp$ is narrow, there is

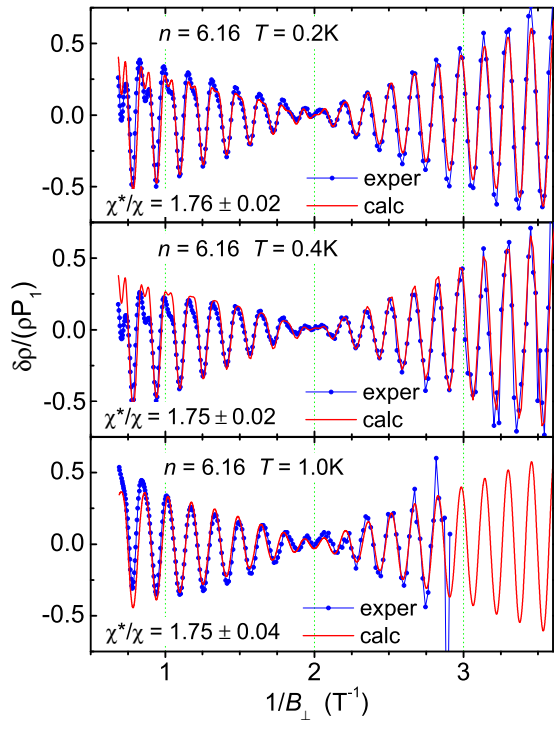

FIG. 2. Examples of the normalized oscillatory magnetoresistance $\delta\rho_{xx}/(\rho_{xx}P_1)$ for high electron density $n = 6.16 \times 10^{11}$ cm^{-2} measured at $B_\parallel = 0.565$ T and three temperatures. Blue dots are the data, blue connecting lines are guides to the eye, and red lines are fitting curves. The extracted from fitting χ^* values and their uncertainty are indicated in each panel. A "small size"sample.

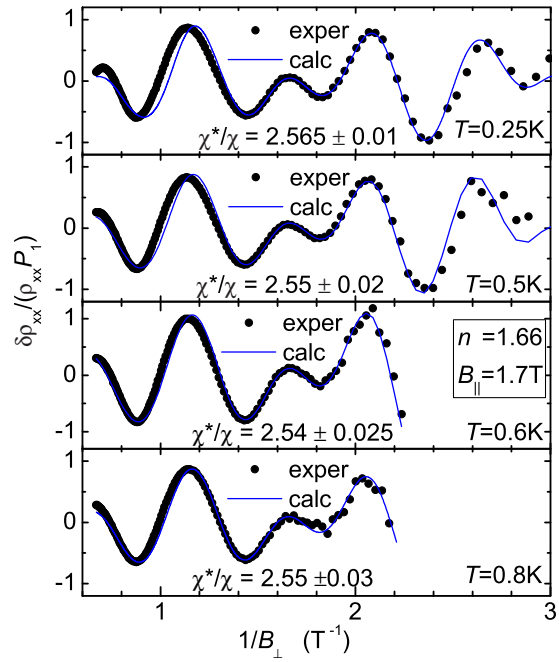

FIG. 3. Examples of the normalized oscillatory magnetoresistance $\delta\rho/(\rho P_1)$ for low electron density and four different temperatures. Dots are the data and blue lines are the fitting curves. The nominal density $n = 1.66 \times 10^{11}$ cm^{-2}, $B_\parallel = 1.7$ T, a "small" sample.

no need in using empirical corrections to the LK formula [70]. We, therefore, were able to fit the data with a single adjustable parameter, χ^*/χ_P.

In stronger magnetic fields, as exemplified in Figs. 2 and 3, at $B_\perp \gtrsim 1$ T, the shape of the oscillations starts to deviate from the LK formula. This is caused by magnetic field dependent variations of screening and level splitting due to the interlevel interaction, the latter is known to be significantly enhanced in the quantum Hall effect regime [71–73]. For this reason, below we analyze only data obtained at $B_\perp \leqslant 1$ T.

The procedure of finding χ^* from the interference pattern is straightforward and does not involve model assumptions; the χ^* value is predominantly determined by the position of the beats and by the phase of the oscillations, which sharply changes by π through the node. For this reason, the uncertainty in the χ^* values is rather small, $\sim 0.5 - 4\%$, which enabled us to detect temperature variations of χ^*.

In general, the accuracy decreases with temperature and reduction in $B_\parallel$, therefore we were able to extract $\chi^*(T)$ only for $T < 1$ K, where ShdH oscillations are clearly resolved in weak $B_\perp$ fields [8,74,75]. Most sensitive to the value of χ^* is the node position in the perpendicular fields $B_\perp \approx 0.5 - 0.6$ T. Therefore, we report χ^* values obtained at such $B_\perp$ fields. In the interval of low electron densities, $n = (1.1 \div 2.2) \times 10^{11}$ cm^{-2}, the main harmonic of the oscillations is suppressed by the Zeeman factor (for more details, see Sec. III D), and the spin splitting causes asymmetric nonharmonic oscillations. This fact favors oscillation analysis and enables extracting χ^* with high precision in very weak and even in zero $B_\parallel$ fields; the representative results are shown in Fig. 4(b).

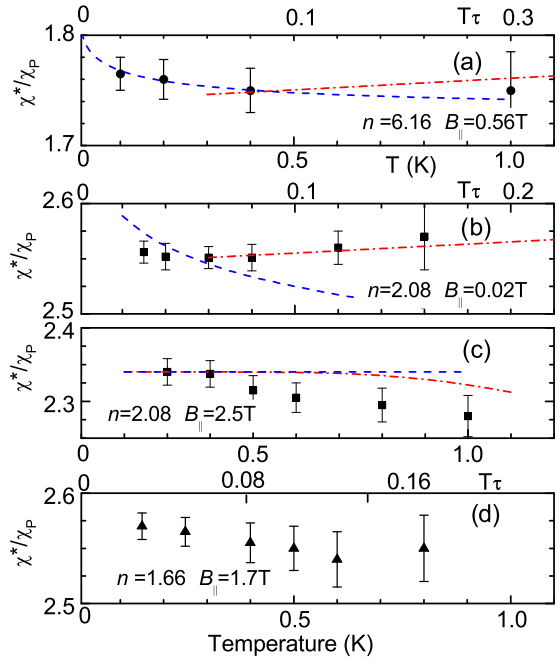

FIG. 4. Temperature dependence of χ^* for a "small" sample with $n_c \approx 1 \times 10^{11}\,\mathrm{cm}^{-2}$ for three densities indicated in units of $10^{11}\,\mathrm{cm}^{-2}$. Upper axes show the temperature in units of $T\tau$. All the data corresponds to $B_\perp \approx 0.3 - 0.6\,\mathrm{T}$; the in-plane field component $B_\parallel$ is indicated in each panel. Dashed and dash-dotted lines show the diffusive and ballistic corrections, respectively. In calculations for panel (a), we used $r_s = 3.35$, $F_0^\sigma = -0.3$, and for (b) and (c), $r_s = 5.77$, $F_0^\sigma = -0.425$ [37]. Diffusive and ballistic corrections were calculated using zero-field expressions Eqs. (2) and (4) for panels (a) and (b), and finite-field Eqs. (A7) and (A8) for panel (c).

We wish to stress that the deduced values of χ^* are independent of details of the fitting, such as, e.g., field dependence of the oscillation amplitude. The χ^* values rely solely on the robust assumption that an in-plane field causes Zeeman splitting of the Landau levels $\hbar\omega_c(n+1/2) \pm g^*\mu_B B_{\mathrm{total}}/2$ which, in its turn, leads to the phase shift between the sequence of the oscillations produced by the "spin-up" and "down" electrons. This method of finding χ^* also relies on the firm fact that the electron-electron interactions in the 2D system affects neither the frequency nor the phase of the oscillations.

Figures 4(a)–4(d) show the obtained-in-this-way temperature dependences of χ^* for three carrier densities. In the explored range of densities, the temperature dependence of χ^* is weak [74]. At even lower densities, close to n_c, χ^* is renormalized significantly. Unfortunately, at such densities, ShdH oscillations can be observed only at the lowest temperatures, and therefore temperature dependence of χ^* is experimentally inaccessible. In the Discussion section, we compare the extracted $\chi^*(T)$ dependence with the theory.

B. Thermodynamic spin susceptibility χ_T

Thermodynamic susceptibility $\chi_\mathrm{T} = dM/dB|_{B=0}$, where M is the magnetization per unit area, was obtained using the recharging technique [59,60,76], in which the chemical potential response $\partial\mu/\partial B$ to a modulation of in-plane magnetic field is measured. By virtue of a Maxwell relation, it can be expressed as a derivative of M with respect to the density: $\partial\mu/\partial B = -\partial M/\partial n$. From the low field slope, $\partial\chi_\mathrm{T}/\partial n = -\partial^2\mu/\partial B^2$ was extracted.

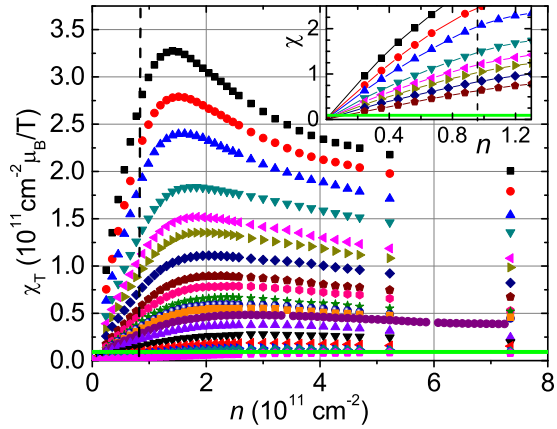

FIG. 5. Thermodynamic spin susceptibility χ_T, determined from the chemical potential variations, versus the carrier density. Different curves correspond to temperatures (from top to bottom) 1.7, 1.8, 2, 2.4, 2.7, 2.9, 3.1, 3.3, 3.5, 3.8, 4, 4.2, 4.6, 5.1, 5.7, 6.9, 8, 9.2, and 13K. Green line shows the Pauli spin susceptibility χ_P. The inset zooms in the same data for the lowest densities and eight temperatures. The dashed vertical line depicts the location of the critical density $n_c \approx 8 \times 10^{10}\,\mathrm{cm}^{-2}$ for the studied sample.

External magnetic field modulation with amplitude $\delta B(\omega)$ at a constant gate voltage leads to a modulation of the charge $\delta Q(\omega)$ given by

$$\delta Q(\omega) = \frac{C(\omega)}{e}\frac{\partial\mu}{\partial B}\delta B(\omega), \tag{5}$$

where $C(\omega)$ is the sample capacitance. It is this charge modulation which is detected in the recharging technique. Extracted from Eq. (5), $\partial\mu/\partial B$ was converted into $\partial M/\partial n$ using the Maxwell relation. The details of this experimental technique have been provided in Refs. [59,60,76]. The thermodynamic susceptibility in principle can be obtained by integration of the low-field slope $d\chi_T/dn = \partial^2 M/\partial n\partial B$ over density

$$\chi(n,T) = \int_0^n \partial\chi/\partial n(n',T)dn'. \tag{6}$$

In practice, the lowest density $n_L(T)$ down to which the recharging technique works is set by the sample and contact resistances, which become large with lowering the density and temperature. Importantly, it was realized [76] that the technique can be used down to the densities substantially below n_c, even though the sample capacitance acquires an imaginary part. Under such conditions, Eq. (5) should be used with the complex capacitance measured at the frequency of the magnetic field modulation.

Although we were able to measure $\partial\chi/\partial n$ down to the densities as low as $4 \times 10^{10}\,\mathrm{cm}^{-2}$ at $T = 1.7\,\mathrm{K}$, still, to integrate we had to extrapolate $\partial\chi/\partial n$ to the interval $0 < n < n_L(T)$. Figure 5 is obtained with $\partial\chi/\partial n$ constant and equal to its value at $n_L(T)$. Taking instead $\partial\chi/\partial n = 0$ in this interval would shift the data in the figure by the value $\chi_\mathrm{T}(n_L)$; this would not lead to a qualitative change of the result.

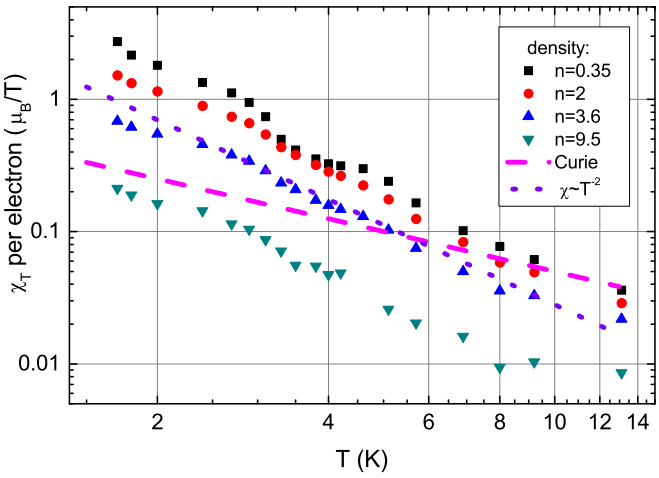

FIG. 6. Temperature dependence of χ_T at different densities plotted for the same data as in Fig. 5. $\chi_T \propto T^{-\alpha}$ with $\alpha \approx 2$. $\chi \propto T^{-2}$ and $\chi \propto T^{-1}$ (the Curie law) are shown for comparison. The fact that $\alpha > 1$ means that the electrons, even at the lowest density, cannot be considered as noninteracting localized ones; this observation lead to the suggestion of the spin droplets in Ref. [59].

In our earlier paper [60], in which the thermodynamic method has been used for the first time, the measurements were performed down to $T = 50$ mK. Treatment of the thermodynamic data in the current paper differs from the previously published results due to different method of integration of $\partial\chi/\partial n$ and $\partial M/\partial n$ over n: in Ref. [60], we integrated starting from a high density, assuming the magnetization at this density to be known. In the current paper, we integrated $\partial M/\partial n$ from a low density. The minimal density $n_L(T)$ down to which we can use this technique increases at low temperatures due to increasing resistance of both the 2DES and the contacts. and no information can be obtained about magnetization at $n = n_c$. This complication is the primary reason to perform the current experiment at ^{4}He temperatures rather than at $T \ll 1$ K. Besides this, we were interested in the low-field behavior, $g\mu_B B \ll k_B T$. Measurements at much lower temperatures would require very weak magnetic fields, which in turn would lead to a small, difficult-to-measure recharging current. Note that the high-field (low-T) measurements have been performed earlier in Refs. [60,61] and they are not the goal of the current paper.

At low densities, χ_T grows linearly with n, which is expected for noninteracting electrons. It reaches a maximum at some density $n(T) > n_c$ and then starts to decrease. We attribute this decrease to melting of the spin droplets with density in the metallic phase. The maximum of $\partial M/\partial n$ and evolution of its position with temperature was discussed in detail in Ref. [59].

The thermodynamic susceptibility χ_T at the lowest temperature of 1.7 K is a factor of 40 greater than the nonrenormalized Pauli susceptibility. As the temperature increases, χ_T strongly decreases as $T^{-\alpha}$ with $\alpha \sim 1-2$, depending on the density, see Fig. 6. This behavior contrasts sharply the weak temperature dependence of the itinerant electrons' susceptibility χ^*. The temperature dependence of χ_T is much stronger than the theory [62,63] predicted for the itinerant electrons. Moreover, it is even stronger than the Curie law $\chi(T) \propto T^{-1}$ expected for noninteracting localized electrons. We, therefore, conclude that χ_T is mainly due to easily polarized localized spin droplets [59], and contribution of the itinerant electrons to χ_T is negligibly small. The fact that $\alpha > 1$ in the $\chi_T(T)$ dependence points at the ferromagnetic type interaction, because random antiferromagnetic interaction results in a spin susceptibility divergence slower than the Curie's low, with $\alpha < 1$ [64].

There is a contradiction between the observed increase of χ_T faster then $1/T$ with decrease of the temperature and the upper bound for the magnetic moment: $M = \mu_B n$. Since χ_T saturates [59,76] at $B_c(T) \propto T$, such divergency would lead to a divergent $M(B_c, T) = \chi_T B_c \propto T^{1-\alpha}$. Therefore, we conclude that this divergency must be cut at a low temperature. This conclusion is in accord with our early measurements [60], which extended down to 50 mK, and in which $\partial M/\partial n$ was limited from above. Unfortunately, at such low temperatures, the accessible range of densities starts from n_c, and therefore one cannot make reasonable assumptions to carry the integration as in Eq. (6).

C. Comparing $\chi^*(T)$ dependence for the itinerant electrons with the interaction corrections

To compare our data with interaction corrections [30], we plotted in Figs. 4(a)–4(c) the diffusive and ballistic interaction corrections. The data is consistent with the corrections at zero and low $B_\parallel$-field, see panels (a) and (b). In particular, there is a qualitative similarity between the data in Fig. 4 and the ballistic corrections (see Fig. 11 of Appendix A). Furthermore, the $\chi^*(T)$ temperature dependence in panels (a) and (b) exhibits a shallow minimum (thought this effect is weak and comparable with the error bars), expected for the ballistic-diffusive crossover [39]. Indeed, as T increases, the diffusive correction decreases χ^* [see Eq. (2)], whereas the ballistic increases [34] [see Eq. (3), and for more details—Appendix A].

The overall explored temperature range, $T\tau \ll 1$, at first sight seems to belong to the diffusive interaction regime. We note, however, that the conventional crossover criterion $T\tau = 1$ is a qualitative estimate. Quantitatively, the crossover temperature calculated for transport [39] is $[(1 + F_0^\sigma)/2\pi\tau]$, i.e., the crossover $T\tau$ value is expected to be $\approx$0.1 for our parameter range. As for the spin susceptibility, the crossover regime has not been calculated until now. Therefore, we plotted in Fig. 4, in addition to the diffusive correction Eq. (A7), also the ballistic one, using Eq. (A8). For weak field [Fig. 4(a)], we compare the data with zero-field theoretical result Eq. (2) rather than with Eq. (A5), since the latter diffusive correction is applicable only above $T = (1 + \gamma_2)g\mu_B B/2\pi \approx 0.5$ K [see Fig. 11(b)], i.e., in the region where predictions of Eqs. (A3) [equivalent to Eq. (2)] and (A5) almost coincide.

Surprisingly, when a strong field, e.g., $B_\parallel = 2.5$ T, which corresponds to $g\mu_B B_\parallel \approx 3K$ [see Fig. 4(c)], is applied, the $\chi^*(T)$ dependence does not vanish [30]. This observation contradicts the interaction correction calculated for diffusive regime, according to which the in-plane field $g\mu_B B_\parallel \gg T$ must cut off the $\chi^*(T)$-dependence, see Eq. (A7). Instead, the temperature dependence of χ^* changes sign, qualitatively

similar to what is expected from ballistic correction (see Appendix A). Quantitatively, $\chi^*(T)$ reduces with temperature somewhat faster than the theory predicts [see Fig. 4(c)]. We note, however, that the uncertainty in the value of prefactor G in Eq. (4) may also be ~ 2, being related to the unknown details of the electron-electron coupling, and with approximations used in deriving Eqs. (4) and (A8).

Importantly, since $\Delta\chi^*(T)$ and $\Delta\sigma(T)$ stem from the same mechanism, according to Ref. [35], they should behave similarly with temperature. Consistent with the theory [39], weakening of the interaction correction to the conductivity $\Delta\sigma(T)$ by $B_\parallel$ field was reported for similar samples [37], therefore the anomalous $\Delta\chi^*(T)$ behavior in strong fields is very surprising. A possible explanation might be that the diffusive-ballistic crossover for $\chi^*(T)$ is shifted down in temperature and corresponds to $T\tau = 0.05 \div 0.1$ rather than unity. It is also worth recalling that we analyzed the ShdH oscillations beatings in the perpendicular field $0.5 \div 0.6$ Tesla. A nonzero magnetic field is predicted [34] to shift the $\chi^*(T)$ minimum to $T = g\mu_B B$ in the ballistic regime. In the data, the minimum, indeed, shifts monotonically to higher temperature with increase of the total magnetic field, which occurs in sequence (b-a-d-c) in Fig. 4. However, the $\chi^*(T)$ minimum according to the ballistic theory should be located at about three times stronger fields.

The above-listed inconsistencies lead us to the conclusion that the temperature dependence of $\chi^*(T)$ in moderately strong magnetic fields, and maybe even to a lesser extent in small fields, is affected by another, stronger mechanism than the FL corrections. This conclusion is supported by thermodynamic data, as will be shown below.

D. Upper bound on χ^* as set by analysis of the magnetooscillations

Above we reported the low-temperature χ^* obtained from the beats of the ShdH oscillation. Unfortunately, this technique cannot be used down to the critical density n_c since the in-plane magnetic field quickly drives the 2D system into an insulator state [27,28,77]. Nevertheless, we still can use ShdH oscillations to set the *limits* for χ^*. For this, we now turn to the analysis of (1) the period and (2) the phase (sign) of ShdH oscillations just above n_c. The period reflects the degeneracy of the system, which would drop by a factor of two if the system becomes fully spin polarized and the Fermi energy doubles. The phase depends on the ratio between the spin and cyclotron splitting, and thus carries information on the degree of spin polarization, $(n_\uparrow - n_\downarrow)/n$.

We first look at the ShdH oscillations, with no $B_\parallel$ applied, at a relatively high density, for which we know χ^* from the oscillation beats. We check that the oscillation frequency and phase (sign) agree with the expectations, and then apply the same analysis to even lower densities for which ShdH beats could not be measured; this will set the upper limit for χ^*.

The logic behind this approach can be understood by examining the schematic energy diagram in Fig. 7. We presume Landau levels to be significantly broadened by scattering, which is definitely true close to n_c. Therefore, in the following, we shall consider the valley splitting to be negligible. When the spin splitting $g^*\mu_B B_{\text{total}}$ is much smaller

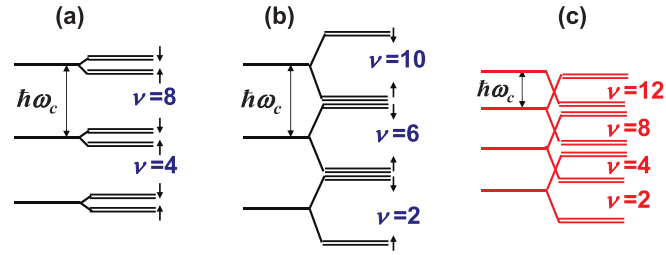

FIG. 7. Evolution of the energy spectrum for the two-valley 2DES in (100) Si-MOS for various Zeeman splittings: (a) $E_Z \ll \hbar\omega_c$, spin splitting is unresolved and $B_\parallel$ field does not affect the oscillations amplitude. (b) $E_Z \lesssim \hbar\omega_c$, spin splitting dominates and increases with the field, causing the oscillations amplitude to grow with $B_\parallel$. (c) $E_Z \approx 2\hbar\omega_c$—this situation does not occur in the studied Si-MOS samples. Unresolved valley splitting is depicted with double lines. Filling factors denote the largest energy gaps.

than the cyclotron energy $\hbar\omega_c$ and therefore unresolved, each Landau level is fourfold-degenerate. The period of the ShdH oscillations corresponds to $\nu = 4$, and $\rho_{xx}(\nu)$ minima are located at $\nu = 4i$ (where $\nu = nhc/eB_\perp$ is the filling factor and i–an integer [6,8,67,68]). This case is illustrated in Fig. 7(a); other cases [Fig. 7(b) and 7(c)] are described in the caption of Fig. 7.

Although the Mermin-Wagner theorem prohibits spontaneous spin polarization at $T > 0$, one may expect to see a strong $\chi^*(T)$ growth as $T \to 0$ in the vicinity of a quantum $(T = 0)$ phase transition to the spin-polarized state. In such a case, a half-period $\Delta\nu = 2$ of the ShdH oscillations would be observed starting from a certain density-dependent in-plane magnetic field. This field would decrease to zero with the density approaching the quantum critical one n_q. Indeed, frequency doubling of the ShdH oscillations induced by a strong external field $B_\parallel \sim 2E_F^*/g^*\mu_B$ was experimentally observed by Vitkalov *et al.* [78].

Using this approach, we now want to test the possibility of anomalous growth of χ^* in a low or zero in-plane field with $n \to n_c$ and show that, if it exists, n_q should be well below n_c. Typical ShdH oscillations of ρ_{xx} for very low densities, close to n_c, are shown in Figs. 8 and 9 as a function of $B_\perp$. Due to high electron mobility, oscillations are detected in $B_\perp$ fields as low as 0.14 T for densities down to n_c (which corresponds to $r_s \approx 9$). The shape of these oscillations cannot be described with LK formula since (i) the electron-electron interactions at such densities are important [70], (ii) close to n_c a 2DEG is at the verge of the hopping regime [79,80], and (iii) at $B_\perp \gtrsim 1$ T the reentrant QHE-insulator transition quickly develops, preventing analysis of oscillations [79,81]. The parameter space where oscillations can be analyzed in the vicinity of n_c is shown in Appendix D. We note that, unless the 2D system is fully polarized, the period of oscillations is robust, since it depends only on the Landau level degeneracy, which is not affected by interactions.

For low densities presented in Fig. 8, Zeeman splitting is comparable to the cyclotron one [see Fig. 7(b)], and, therefore, the $\rho(B_\perp)$ minima in Fig. 8(a) are due to the spin gaps [7,8,82,83]. Figure 8(b) shows that the magnitude of the oscillations increases with in-plane magnetic field $B_\parallel$, which

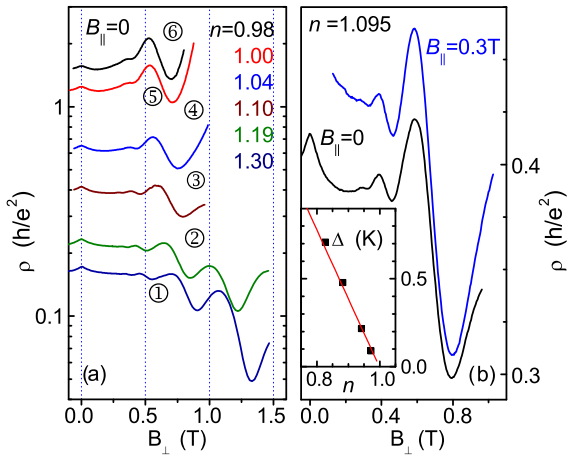

FIG. 8. (a) ShdH oscillations for a "small" sample at six densities near $n_c \approx 1.0 \times 10^{11}$ cm^{-2}, $T = 0.2$ K. Curves $3-6$ are terminated at the onset of the large insulating peak in ρ [79]. (b) Enhancement of oscillations with $B_\parallel$. The inset in panel (b) illustrates the determination of the critical density from the activation energy Δ, similar to Refs. [79,80]. Densities are given in units of 10^{11} cm^{-2}.

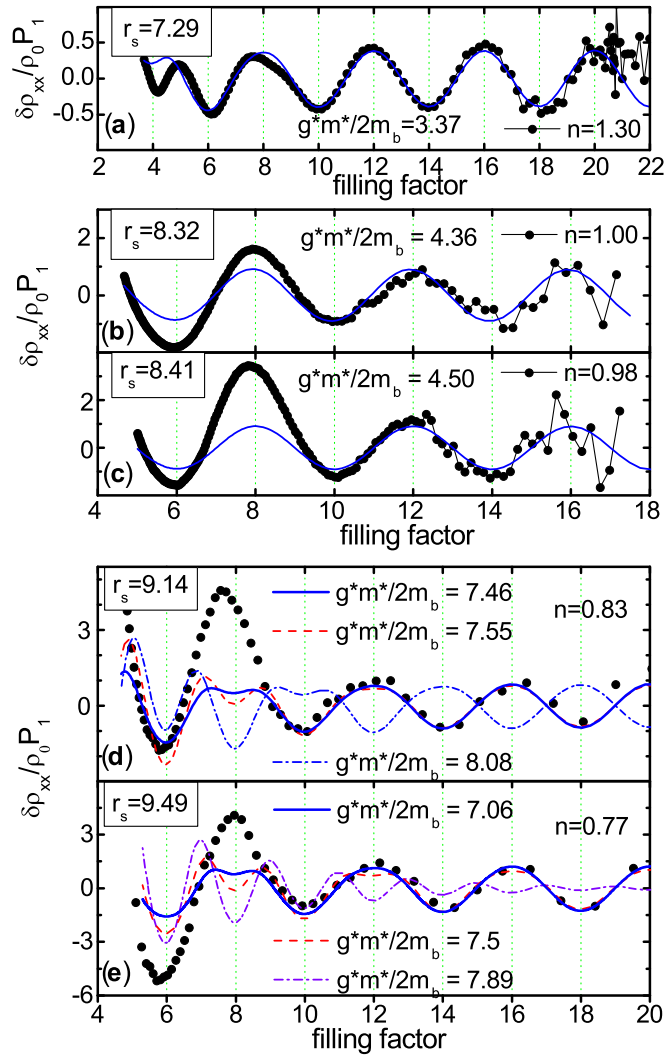

FIG. 9. Oscillatory component of the resistivity $\Delta\rho(\nu)/\rho_0 P_1$ in $B_\parallel = 0$. (a)–(c) 'Small" sample with data *1, 5*, and *6* from Fig. 8(a), $n_c = 1.0 \times 10^{11}$ cm^{-2}. (d), (e) 'Large" sample with $n_c = 0.77 \times 10^{11}$ cm^{-2}. Dots are the data, fits are the lines [8] with parameters shown in the panels. The temperature is 0.2 K for panels (a)–(c) and 0.03 K for panels (d) and (e). The values of n are in units of 10^{11} cm^{-2}. The red dashed and blue dashed-dotted lines in panels (d) and (e) show what happens to the oscillation shape if one uses inappropriate (increased) values of the fitting parameter $(g^*m^*/2m_e) \propto (\chi^*/\chi_P)$.

enhances only spin splitting. The increase in the magnitude confirms that the ratio of the Zeeman energy $E_Z = g^*\mu_B B_{\rm total}$ to the cyclotron energy $\hbar\omega_c$ lies within the interval $1/2 < E_Z/\hbar\omega_c < 1$ [see Fig. 7(b)]. This estimation is obtained from the oscillation phase in the density range $r_s = 6.3-8.2$; it is in good agreement with our earlier quantitative measurements of $\chi^*(n)/\chi_b \approx 5-6$ [8] from the beating pattern of the ShdH oscillations in low crossed fields.

Curve *5* in Fig. 8(a) corresponds to the density $n = n_c$. The latter value was determined by extrapolating the density dependence of the activation energy $\Delta(n)$ for the exponential temperature dependences $\rho \propto \exp(\Delta/T)$ in the insulating regime to zero [79,80,84]; this procedure is illustrated in the inset to Fig. 8(b).

To clearly illustrate the phase (sign) and period of ShdH oscillations in the low-field range, we present in Fig. 9 the $\Delta\rho_{xx}/\rho_0 P_1$ data obtained at $B_\parallel = 0$ as a function of the Landau level filling, $\nu = nh/eB_\perp$; the data is normalized by the calculated amplitude of the first ShdH harmonic $P_1(B_\perp)$ [8,67]. In calculating P_1, we used the values of $g^* \propto \chi^*(n)/m^*$ and $m^*(n)$ measured in Refs. [8,37]. The Dingle temperature, T_D [see Eq. (B1)] was adjusted to match damping of the measured oscillations in weak fields.

In strong fields, the oscillations amplitude is not described by LK formula, and is enhanced due to the factors mentioned above. Nevertheless, even in this case we obtain a reliable estimation of χ^*, since we rely solely on the oscillation period and phase, rather than the oscillations amplitude.

As seen from Fig. 9, down to the critical density for both samples, $n \approx 1 \times 10^{11}$ cm^{-2} for the small one (panels a-b-c) and $n = 0.77 \times 10^{11}$ cm^{-2} for the large one (panels d-e), the period of ShdH oscillations in weak $B_\perp$ fields (large fillings) remains equal to $\Delta\nu = 4$ providing evidence for the system to be unpolarized. T illustrate this even further, we show in panels (d) and (e) a simulation with χ^* increased by 6% (dashed line) and 12% (dash-dotted line); the appearance of the second harmonic and the change of oscillation phase by π that would be caused by such an increase is clearly visible. From this we conclude that χ^* value cannot be increased even by a relatively small factor.

In the analysis of ShdH oscillations, it is important to limit the field range to $B_\perp \leqslant 1$ T in order to avoid (i) *the magnetic-field-induced spin polarization* and (ii) *the emerging reentrant quantum Hall effect-to-insulator transitions* [79,81]. This limitation is violated at about $\nu = 5$: a shift of the minimum at $\nu \approx 4$ in Fig. 9(a) is caused by reason (i), i.e., by partial lifting of the spin degeneracy in perpendicular field $B_\perp \approx 1.3\,T$. In Figs. 9(b)–9(e), this limitation is also violated

for $\nu < 10$ and reason (ii) may account for the excessive oscillation amplitude (for more details, see Appendix D).

We now consider the phase (sign) of the oscillations. The minima of $\Delta\rho$ in Fig. 9 are located at $\nu = 6, 10, 14, 18$, i.e., at $\nu = (4i - 2)$, in contrast to $\nu = 4, 8, 12, 16$, i.e., $\nu = 4i$, as observed for higher densities. In other words, the phase of the oscillations at low densities is reversed. The position of the oscillations minima is consistent with earlier studies [79,82,83], with values of χ^* measured from the oscillations beating [8], and with the above analysis of the oscillation period (Fig. 9). Schematically, the energy spectrum for such a situation, $E_Z \gtrsim \hbar\omega_c^*$, is shown in Fig. 7(b). The oscillation phase changes by π (i.e., sign changes) due to the Zeeman factor $\cos(\pi E_Z/\hbar\omega_c)$ when E_Z exceeds $\hbar\omega_c^*/2$, i.e., when χ^*/χ_P becomes equal to $1/2$, which occurs at $r_s > 6.3$ [8,67], as schematically illustrated in Figs. 7(a) and 7(b). The sign change is fully consistent with other observations (see, e.g., Refs. [82,83]).

Since the phase of the ShdH oscillations is determined by the ratio of the Zeeman to cyclotron splitting [67,69],

$$\cos\left(\pi\frac{g^*\mu_B B}{\hbar\omega_c^*}\right) = \cos\left(\pi\frac{\chi^*}{\chi_P}\frac{m_b}{m_e}\right), \tag{7}$$

it was concluded in Ref. [85] that, to have π phase shift in the range $10 > r_s > 6$, the spin susceptibility χ^* must obey the following inequality: $2.6 = m_e/2m_b < \chi^*/\chi_P < 3m_e/2m_b = 7.9$. This inequality, together with a vanishingly small $\chi^*(T)$-dependence sets constrains on the value of χ^* at the MIT critical density.

The above analysis of the period and phase of oscillations provides strong evidence for the absence of complete spontaneous spin/valley polarization of the itinerant electrons at the sample-dependent MIT critical density $n \geqslant 0.98 \times 10^{11}\,\mathrm{cm}^{-2}$ (for a "small" sample) and $n \geqslant 0.77 \times 10^{11}\,\mathrm{cm}^{-2}$ (for a "large" sample).

Another scenario, a potential divergence of χ^* and m^* for itinerant electrons at a sample-independent density n_0 was explored in Ref. [85] by scaling the $\chi^*(n - n_0)$ dependence. It was found that the $\chi^*(n) \propto g^*m^*$ data for both samples (the "large" and "small" ones) obey a common critical dependence only if we choose $n_0 < 0.53 \times 10^{11}\,\mathrm{cm}^{-2}$, the unrealistically low value that belongs to the insulating regime.

This conclusion differs from the one suggested in Refs. [13,15]. A possible reason for this disagreement is magnetization nonlinearity: strong magnetic field, as used in Refs. [13,15], drives the system near n_c into the insulator [86]. As was pointed out in Ref. [87], the MR data for in-plane fields, analyzed in Refs. [13,15], is only approximately related to the spin susceptibility of *itinerant* electrons, because it ignores the magnetic field dependence of χ even in the "metallic" conduction regime [10].

E. Spin polarization probed by the thermodynamic χ_T measurements

After setting the upper bound on the degree of spin polarization of the itinerant electrons for $T \to 0$, we shall discuss the polarization of the whole system measured with recharging technique.

In the same way as χ_T was obtained by integration of $\partial\chi/\partial n$, we obtained $M(B)$ by integration of $\partial M/\partial n$ at different magnetic fields and temperatures. The results for $T = 1.7\,\mathrm{K}$ are shown in Fig. 10. The magnetic moment of the system as a whole grows linearly with the field, thus excluding zero-field spin polarization. Indeed, if it existed, it would lead to an offset: a finite M at $B \to 0$. At low densities below $n_c = 8 \times 10^{10}\,\mathrm{cm}^{-2}$ for the "large" high mobility sample, the magnetic field of 0.5 T almost polarizes the system. When the density increases above n_c, the magnetic moment at saturation stops to grow with n, and even somewhat decreases.

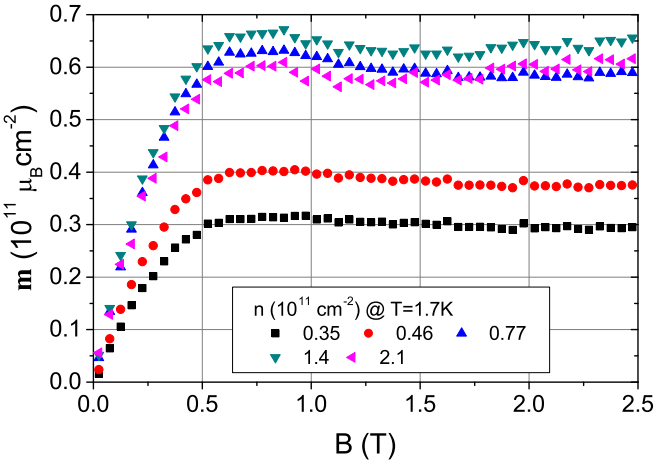

FIG. 10. Magnetic field dependence of the sample magnetization M at $T = 1.7\,\mathrm{K}$ and several densities. M is linear in B in weak fields, and saturates at values below full polarization. Decrease of M with increasing B can be attributed to inaccuracy of subtracting the diamagnetic contribution to $\partial M/\partial n$[76]. The data for a "large" sample.

At some temperature-dependent density, close but above n_c, sample magnetization starts to decrease with density: e.g., magnetization for $n = 2.1 \cdot 10^{11}\,\mathrm{cm}^{-2}$ is smaller than magnetization for $n = 1.4 \cdot 10^{11}\,\mathrm{cm}^{-2}$ This is consistent with the nonmonotonic density dependence of χ_T shown in Fig. 5. There is also a slight decrease of magnetization with magnetic field above $B \approx 0.7\,\mathrm{T}$. We attribute it to inaccuracy of subtraction of the diamagnetic contribution: this contribution, being unimportant at weak magnetic fields, becomes important at strong, at which the paramagnetic contribution saturates.

Finally, we note that the exponent α in the temperature dependence of χ_T in Fig. 6 shows no critical behavior at $n = n_c$: it increases monotonically with decrease of the density. In Refs. [61,88], the opposite conclusion was drawn from similar measurements of χ_T by erroneously identifying the densities at which χ_T reaches maxima (see Fig. 5) with the onset of full spin polarization, see Ref. [89] for discussion.

III. CONCLUSIONS

To summarize, we found that:

(1) Spin susceptibility χ^* of itinerant electrons in a strongly correlated 2D electron system in Si inversion layer weakly depends on temperature over the range $0.05-1\,\mathrm{K}$.

(2) This weak $\chi^*(T)$-dependence does not support non-FL predictions for the power-law divergence of χ^* as $T \to 0$.

(3) The temperature dependence of χ^* in low magnetic fields is consistent with the FL interaction corrections. In contrast, the temperature dependence of χ^* in the magnetic field $B_\parallel > T/\mu_B$ seems somewhat stronger than the interaction correction in ballistic regime predicts; on the other hand, it does not vanish, as expected for the interaction correction in diffusive regime.

(4) The above inconsistencies might stem from the fact that the diffusive-ballistic crossover in the susceptibility sets at temperature much lower than the conventional $T = 1/\tau$ value.

(5) Thermodynamic spin susceptibility χ_T is much larger than χ^*, and its temperature dependence is much stronger. We attribute this large susceptibility to the localized spin droplets [59]. Their contribution to thermodynamics, and, particularly, to the spin susceptibility of the two-phase state is dominant; it is magnetic field and temperature dependent and, therefore, may also affect the $\Delta\chi^*(T, B)$ dependence observed in our experiments in in-plane magnetic fields.

(6) The striking difference of the weak $\chi^*(T)$ and strong $\chi_T(T)$ dependences is evidence for a two-phase state consisting of easily polarisable spin droplets and an FL, even for the well conducting "metallic" regime $k_F l \gg 1$.

(7) By analyzing both thermodynamic and transport data, we exclude the possibility of a magnetic instability in Si 2DES at any density above $5.3 \times 10^{10}\,\mathrm{cm}^{-2}$, including the MIT critical density $n = n_c$. The complete spin polarization is absent both in zero and low fields, in the accessible range of temperatures (down to 100 mK).

We conclude that the FL type interaction corrections describe the measured $\chi^*(T)$ dependence for itinerant electrons reasonably well. The observed deviations from the FL picture may be caused by the presence of the polarized spin-droplets, whose coexistence with the FL-state is evidenced by the thermodynamic magnetization data. In general, interacting electron systems often have a tendency to phase separation in the vicinity of the MIT [90] or superconductor-insulator transition [91,92]. The concept of the 2D electron liquid as the two-phase state [56,57,93] is capable of qualitatively explaining thermodynamic magnetization data. The quantitative description of $\chi_T(T)$ and $\chi^*(T)$ dependences, and, particularly, understanding the crossover regime in $\chi^*(T)$, however, requires further studies.

ACKNOWLEDGMENTS

Authors are grateful to B. L. Al'tshuler, A. V. Chubukov, D. V. Efremov, A. M. Finkel'stein, D. L. Maslov, O. Sushkov, and A. Yu. Zyuzin for discussions, and to N. Teneh for his assistance in thermodynamic magnetization measurements. V.M.P. is supported by RFBR No. 18-02-01013 (measurements) and by Russian Ministry of Education and Science (Project No. 2017-14-588-0007-011), A.Yu. K. is supported by Basic research program of the HSE, ISB is partially supported by the program 0033-2018-0001 "Condensed Matter Physics" and by the Alexander von Humboldt Foundation. I.S.B. and M.R. acknowledges Israeli Science Foundation, and M.G. the NSF Grant DMR No. 0077825. Measurements were partly done using research equipment of the Shared Facility Center at LPI.

APPENDIX A: INTERACTION CORRECTIONS TO $\chi^*(B, T)$

In this appendix, we discuss briefly theoretical background for the interaction corrections to the spin susceptibility $\chi^*(B, T)$ in the diffusive and ballistic regimes.

1. Diffusive regime

The original Al'tshuler-Zyuzin result [30] predicts the following behavior of the spin susceptibility of a disordered 2D electron system in the diffusive regime:

$$\Delta\chi(T) \propto -\begin{cases}\ln(T\tau), & B_\parallel = 0,\\ \ln(g\mu_B B_\parallel \tau), & g\mu_B B_\parallel \gg T.\end{cases} \tag{A1}$$

Extension of the original result of Ref. [30] to an arbitrary value of the ratio $g\mu_B B_\parallel/T$ and an arbitrary number of valleys, n_v can be done under the following assumptions: (i) the system is in the metallic regime, i.e., zero-field conductivity is large, $\sigma_{xx}(0) \gg e^2/h$; (ii) the temperature is low enough: $(1+\gamma_2)T\tau \ll 1$; and (iii) the parallel magnetic field is not too strong $(1+\gamma_2)g\mu_B B_\parallel \tau \ll 1$. Here, we remind that parameter γ_2 determines FL renormalization of g-factor, $g^* = (1+\gamma_2)g$, and can be expressed through the temperature-independent FL parameter F_0^σ: $\gamma_2 = -F_0^\sigma/(1+F_0^\sigma)$. For the representative density $2 \times 10^{11}\,\mathrm{cm}^{-2}$ the parameter $\gamma_2 \approx 0.6$. Following the approach of Refs. [94,95], one can find

$$\frac{\chi(B_\parallel)}{\chi(0)} = 1 - \frac{1}{\sigma_{xx}(0)}\frac{n_v^2(1+\gamma_2)}{\pi^2}\mathcal{F}\left(\frac{g\mu_B B_\parallel}{2\pi T}\right). \tag{A2}$$

Here (0) stands for zero field, and $\sigma_{xx}(0)$ is in units of $e^2/\hbar$:

$$\frac{\chi(0)}{\chi_P} = \left[1 + \frac{1}{\sigma_{xx}(0)}\frac{n_v^2\gamma_2}{\pi^2}\left(\ln\frac{1}{2\pi T\tau} - \psi(1)\right)\right], \tag{A3}$$

and the function $\mathcal{F}$ is expressed through the Euler di-gamma function:

$$\mathcal{F}(h) = \mathrm{Re}\left[\psi(1 + i(1+\gamma_2)h) - \frac{\psi(1+ih) + \gamma_2\psi(1)}{1+\gamma_2}\right]. \tag{A4}$$

We emphasize that Eqs. (A2) and (A3) are derived to the lowest order in $1/\sigma_{xx}(0)$ (in the dimensionless units, as stated above).

At weak fields and not too low temperatures, $(1+\gamma_2)g\mu_B B_\parallel/(2\pi T) \ll 1$, one can expand the function $\mathcal{F}(h)$ to the second order in h, and find

$$\frac{\chi(B_\parallel)}{\chi(0)} = 1 - \frac{1}{\sigma_{xx}}\frac{\zeta(3)}{\pi^2}n_v^2[(1+\gamma_2)^3 - 1]\left(\frac{g\mu_B B_\parallel}{2\pi T}\right)^2. \tag{A5}$$

In the opposite limit of low temperatures, $2\pi T \ll (1+\gamma_2)g\mu_B B_\parallel$, we obtain the following asymptotic behavior:

$$\frac{\chi(B_\parallel, T)}{\chi(0)} = 1 - \frac{1}{\sigma_{xx}}\frac{n_v^2\gamma_2}{\pi^2}\left[\ln\frac{g\mu_B B_\parallel}{2\pi T} - \psi(1) + \frac{1+\gamma_2}{\gamma_2}\ln(1+\gamma_2)\right]. \tag{A6}$$

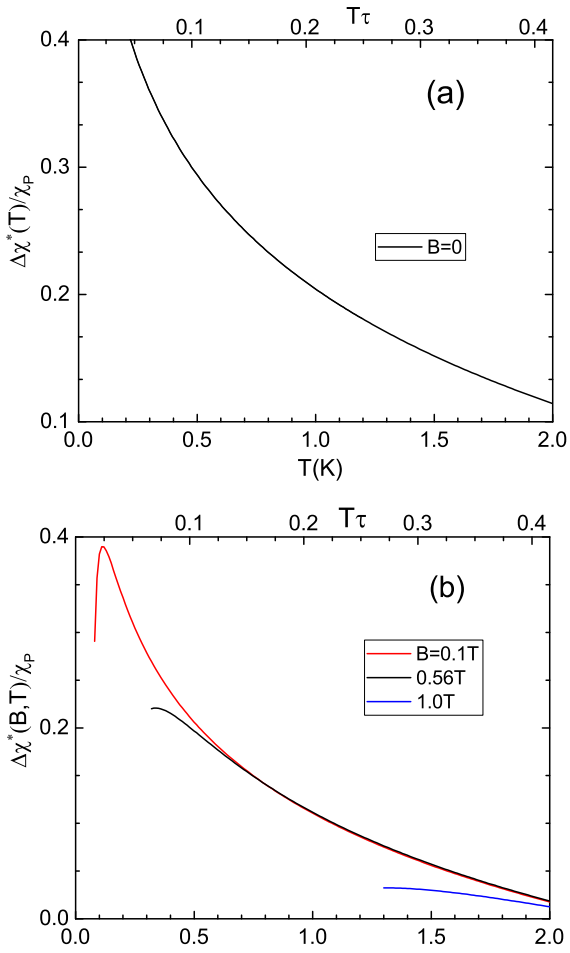

FIG. 11. Temperature dependence of the diffusive interaction correction $\Delta\chi^*(T)$ for parameters corresponding to Fig. 4(b): $n = 2.08 \times 10^{11}\,\mathrm{cm}^{-2}$, $\tau = 1.59\,\mathrm{ps}$, $F_0^\sigma = -0.38$, $\gamma_2 = 0.61$, "small" sample. (a) Calculated from Eq. (A3) for $B = 0$; temperature interval is cut by requirements $\Delta\chi^*(T)/\chi_P < 0.4$ ($T \geqslant 0.05\,\mathrm{K}$), and $T\tau < 0.42$ ($T < 2\,\mathrm{K}$). (b) Calculated from Eq. (A5) for $B = 0.1$, 0.56 and 1.0 T. For panel (b), temperature is limited from below by the requirement $(1+\gamma_2)g\mu_B B_\parallel/(2\pi T) < 1$, and from above, by $T\tau < 0.42$ ($T < 2\,\mathrm{K}$). Vertical position is chosen to obtain vanishing $\Delta\chi^*(T)$ for $T\tau = 1$.

This result implies

$$\frac{\chi(B_\parallel) - \chi_P}{\chi_P} \approx -\frac{1}{\sigma_{xx}}\frac{n_v^2\gamma_2}{\pi^2}\ln(g\mu_B B_\parallel \tau), \qquad \text{(A7)}$$

that is perfectly consistent with the well-known result, Eq. (A1) [30].

In Fig. 11, we show the $\Delta\chi(B_\parallel, T)$ dependences calculated from Eq. (A3) for $B_\parallel = 0$ and from Eqs. (A5) and (A6) for $B_\parallel = 0.1$, 0.5 T and 1 T. Note that $(1+\gamma_2)g\mu_B B_\parallel \tau$ becomes unity at $B \sim 2.3\,\mathrm{T}$ (τ is indicated in the upper horizontal scale of Figs. 4(a)–4(d), and is also given in the captions to Fig. 11), so that assumption (iii) of its smallness is violated for experimental parameters of Fig. 4(d), and to some extent, of Fig. 4(c). In such high fields, Eq. (A7), according to which χ^* is temperature independent, is more appropriate.

The logarithmic increase of $\Delta\chi^*$ with lowering temperature comes from $\chi(0)$, Eq. (A5). The maximum and the further decrease seen at very low temperatures (and not observed in the experiment) for $B_\parallel = 0.1\,\mathrm{T}$ comes from the field-dependent correction in Eqs. (A5) and (A6).

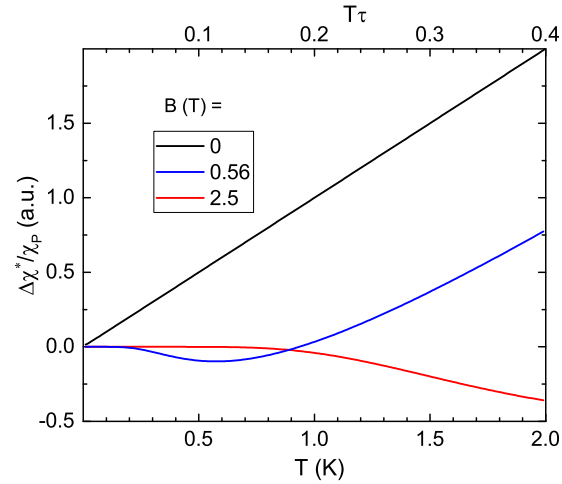

FIG. 12. Ballistic correction $\Delta\chi^*(T)/\chi_P$ calculated from Eq. (A8) of Ref. [34] for parameters corresponding to Figs. 4(a)–4(c): $n = 2.08 \times 10^{11}\,\mathrm{cm}^{-2}$, $\tau = 1.59\,\mathrm{ps}$, the "small" sample, at $B = 0$, 0.56, and 2.5 T. Vertical scale is the same for all three curves. Upper scale shows temperature in units of $T\tau$.

2. Ballistic regime

For completeness, we remind of the result for the interaction correction to the spin susceptibility $\Delta\chi^*(T) = \chi^*(T) - \chi^*(0)$ in the ballistic regime, $T\tau \gg 1$. At zero field, $\Delta\chi^*(T)$ for a 2D system increases approximately linear with T (see Eq. (3) and Refs. [31–36]). This linear in T dependence appears in the second order in the interaction corrections due to nonanalytic behavior of the polarization operator at $q = 2k_F$. In Ref. [34], the correction to the spin susceptibility was computed in the presence of a nonzero in-plane magnetic field. The result is the following:

$$\Delta\chi^*(T) = \chi_P A^2(\pi) T f(g\mu_B B_\parallel/T), \qquad \text{(A8)}$$

where

$$f(x) = \frac{x}{\sinh^2(x)}[\sinh(2x) - x], \qquad \text{(A9)}$$

and $A \sim 1$. TO compare this prediction with the experimental data in Figs. 4(a)–4(c), we show in Fig. 12 $\Delta\chi^*(T) = \chi^*(T) - \chi^*(0)$ dependence calculated from Eq. (A8) for $B_\parallel = 0$, 0.56, and 2.5T. Though there is a certain similarity, the whole explored temperature range formally belongs to the diffusive interaction regime $T\tau \ll 1$ and the applicability of the ballistic corrections (Fig. 12) to the data, Fig. 4 is questionable.

APPENDIX B: EXPERIMENTAL DETERMINATION OF THE CARRIER DENSITY

The *full carrier density* n in the 2D channel of Si-MOSFETs was determined from the ShdH oscillations and from the Hall effect measurements. Both methods are applicable down to the critical density $n_c \approx 1 \times 10^{11}\,\mathrm{cm}^{-2}$, and give

the same results with accuracy of a few percent [13]. Within the same accuracy, these results also agree with the charge in the gated Si-MOSFET directly measured by recharging or capacitive-type techniques [96]:

$$n = \frac{C}{Se}(V_g - V_{th}).$$

Here V_{th} is the gate voltage at which density extrapolates to zero and S is the sample area. The calculated value of capacitance C agrees with the directly measured capacitance of the sample.

Density of itinerant and localized electrons.

We presume the itinerant electrons to be those having a *ps*-scale relaxation time and therefore providing a dominant contribution to the DC conductance and ShdH. In contrast, the localized carriers are trapped for a much longer time, and their contribution to the conductivity is negligible. Both ShdH and Hall effect measurements give results close to the full electron density. At high densities deep in the metallic phase and at low magnetic fields in a uniform system all electrons are itinerant, and $n_i = n$.

In a nonuniform system, ShdH and Hall effect also measure the full electron density. ShdH counts the number of filled Landau levels, without distinguishing between localized and extended states, an extreme example is the QHE: there might be a few extended states in the middle of the Landau levels, but the density extracted from the oscillations period is just the full one, n. In the QHE case, the Hall effect is stepwise; the width of the steps is an indication for the number of localized states in this regime. The density of localized states is known to oscillate with filling factor or Fermi energy position relative to the Landau levels. We are not aware of a straightforward way to infer the number of localized electrons in low magnetic fields close to the MI transition. Our measurements of the number of the easily polarized spins can be an indication.

Anyhow, the knowledge of n_i at different scales is not required for the subject of this paper: namely, the susceptibility and its properties with n and T being the governing parameters.

APPENDIX C: FITTING OF THE SHDH OSCILLATIONS

The magneto-oscillations in the *noninteracting* Fermi gas are usually fitted [8,70] by the LK formula, adapted for the 2D case and valid for a small amplitude of oscillations $\delta\rho/\rho \ll 1$ [67] :

$$\frac{\delta\rho_{xx}}{\rho_0} = +2\frac{\Delta D}{D} = \sum_i A_i^{\mathrm{LK}} \cos\left[\pi i\left(\frac{\hbar c\pi n}{eB_\perp} - 1\right)\right] Z_i^s Z_i^v.$$

$$A_i^{\mathrm{LK}} = 4\exp\left(-\frac{2\pi^2 i k_B T_D}{\hbar\omega_c}\right)\frac{2\pi^2 i k_B T/\hbar\omega_c}{\sinh(2\pi^2 i k_B T/\hbar\omega_c)}. \quad \text{(C1)}$$

Here $\omega_c = eB_\perp/m^*c$ is the cyclotron frequency, D is the 2D density of states, T_D is the Dingle temperature, and the Zeeman- and valley-splitting terms are

$$Z_i^s = \cos\left[\pi i\frac{\hbar\pi P c n}{eB_\perp}\right], \quad Z_i^v = \cos\left[\pi i\frac{\Delta_V}{\hbar\omega_c}\right], \quad \text{(C2)}$$

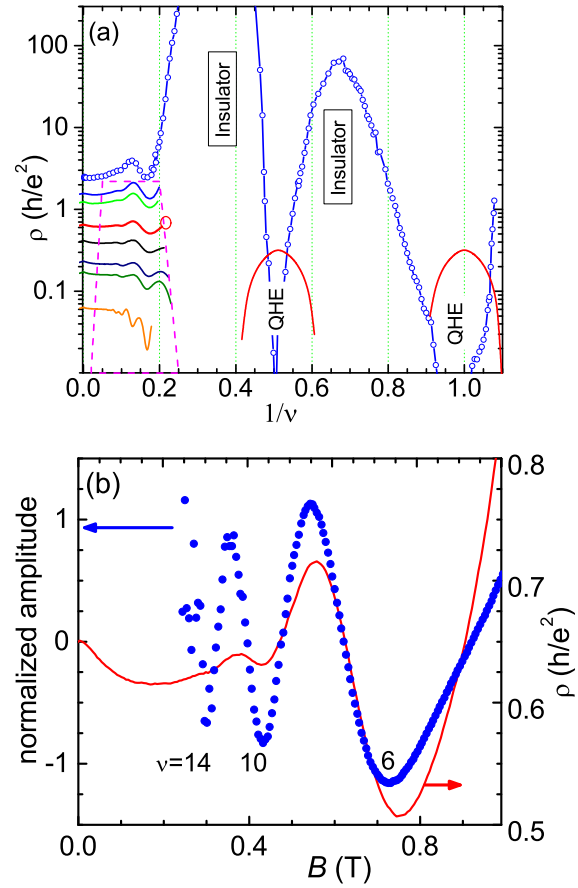

FIG. 13. Evolution of the ShdH oscillations at different densities close to the critical density of MIT for the "small" sample ($n_c \approx 0.97 \times 10^{11}$ cm^{-2}). Empty circles in panel (a) show the ρ_{xx} oscillations at $n \approx 0.97 \times 10^{11}$ cm^{-2}, which in high fields are transformed into the reentrant QHE-insulator transitions [79]. Dashed line confines the region of our weak field ShdH measurements in Ref. [85]. The oscillatory curves in the confined regions are for densities (from top to bottom) 0.98, 0.99, 1.04, 1.10, 1.20, 1.30, and 1.98 in units of 10^{11} cm^{-2}. (b) Right axis: expanded view of one of the $\rho_{xx}(B)$ curves at $n = 1.04 \times 10^{11}$ cm^{-2} [marked with a circle on panel (a)]; left axis: the MR oscillatory component after subtraction the monotonic magnetoresistance and normalization by the amplitude of the first harmonic $P_1(B_\perp)$ [8].

where $P = (n_\uparrow - n_\downarrow)/n$ is the spin polarization, $n_\uparrow$ ($n_\downarrow$) stand for the density of spin-up (spin-down) electrons, and Δ_V is the valley splitting [6].

In the absence of in-plane field, the Zeeman term reduces to the field-independent factor:

$$\cos\left(\pi i\frac{\Delta_Z}{\hbar\omega_c}\right) = \cos\left(\pi i\frac{g^*m^*}{2m_e}\right).$$

In the case of *interacting* electrons, the temperature dependence of the oscillation amplitude changes [70,97,98]. The modified amplitude of the oscillations is a monotonic function of $B_\perp$ [70] and its exact shape does not affect fitting in the narrow field interval in the vicinity of the nodes (Fig. 2).

APPENDIX D: DOMAIN OF MEASUREMENTS OF THE SHDH OSCILLATIONS CLOSE TO n_c

Figure 13(a) illustrates the parameter range, in which the quantum oscillations were measured in the vicinity of the insulating regime. For a density close to n_c, as the perpendicular field increases, the 2D system experiences reentrant QHE-insulator transition (see Refs. [79,82]). In weaker fields, however, the oscillations look quite ordinary, enabling their conventional analysis, as we described above.

The oscillation amplitude in Fig. 13(b) is damped by a factor of $\sim 1/50$ in the field of $B_\perp = 0.4\,\mathrm{T}$; converting this "Dingle factor" to the quantum (all angle) scattering time $\tau_q = \hbar/2\pi k_B T_D$, we conclude that the 2D system approaches critical density with rather high $\omega_c\tau_q \sim 1$ value in $B_\perp = 0.4T$. On the other hand, treating the DC conduction with Drude formula, we find the momentum relaxation time to be several times smaller. The fact that τ_q exceeds the momentum scattering time τ when n approaches n_c is puzzling, though well known. Its discussion is beyond the framework of the current paper; we only note that such unusual relation between the scattering times indicates failure of the homogeneous FL state and may be understood within the concept of the two-phase state [56,59].

[1] E. M. Lifshits and L. P. Pitaevskii, *Statistical Physics, Part II: Theory of the Condensed State*, L. D. Landau Course of Theoretical Physics, Vol. IX (Pergamon Press, Oxford, New York, 1986).

[2] D. Pines and P. Nozieres, *The Theory of Quantum Liquids* (Benjamin, New York, 1996).

[3] L. D. Landau, Zh. Eksp. Teor. Fiz. **30**, 1058 (1956) [Sov. Phys. JETP **3**, 920 (1957)].

[4] A. A. Abrikosov, L. P. Gorkov, and I. E. Dzyaloshinski, *Methods of Quantum Field Theory in Statistical Physics* (Dover Publications, New York, 1963).

[5] The parameter $r_s = 2.63 \times (10^{12}\,\mathrm{cm}^{-2}/n)^{1/2}$ which characterizes the electron-electron interactions, is the ratio of the Coulomb interaction energy E_{ee} to the Fermi energy E_F. The bare values of the Fermi energy E_F, the effective mass $m_b = 0.19$, and the dielectric constant $\kappa = 7.8$ at the Si-SiO_2 interface are used in its definition.

[6] T. Ando, A. B. Fowler, and F. Stern, Rev. Mod. Phys. **54**, 437 (1982).

[7] T. Okamoto, K. Hosoya, S. Kawaji, and A. Yagi, Phys. Rev. Lett. **82**, 3875 (1999).

[8] V. M. Pudalov, M. E. Gershenson, H. Kojima, N. Butch, E. M. Dizhur, G. Brunthaler, A. Prinz, and G. Bauer, Phys. Rev. Lett. **88**, 196404 (2002).

[9] J. Zhu, H. L. Stormer, L. N. Pfeiffer, K. W. Baldwin, and K. W. West, Phys. Rev. Lett. **90**, 056805 (2003).

[10] V. M. Pudalov, M. E. Gershenson, and H. Kojima, in *Fundamental Problems of Mesoscopic Physics*, NATO Science Series, Vol. 154, edited by I. Lerner, B. Altshuler, and Y. Gefen, 309 (Kluwer Academic Publishers, Dordrecht, the Netherlands, 2004).

[11] E. Tutuc, S. Melinte, and M. Shayegan, Phys. Rev. Lett. **88**, 036805 (2002).

[12] W. R. Clarke, C. E. Yasin, A. R. Hamilton, A. P. Micolich, M. Y. Simmons, K. Muraki, Y. Hirayama, M. Pepper, and D. A. Ritchie, Nat. Phys. **4**, 55 (2008).

[13] A. A. Shashkin, S. V. Kravchenko, V. T. Dolgopolov, and T. M. Klapwijk, Phys. Rev. Lett. **87**, 086801 (2001).

[14] M. P. Sarachik and S. A. Vitkalov, J. Phys Soc. Jpn. Suppl. A **72**, 53 (2003).

[15] S. A. Vitkalov, H. Zheng, K. M. Mertes, M. P. Sarachik, and T. M. Klapwijk, Phys. Rev. Lett. **87**, 086401 (2001).

[16] A. M. Finkelstein, Sov. Sci. Rev. Sec. A **14**, 3 (1990).

[17] For reviews, see: G. Senatore, S. Moroni, and D. Varzano, Solid State Commun. **119**, 333 (2001); A. Isihara and L. C. Ioriatti, Jr., Phys. Rev. B **25**, 5534 (1982).

[18] W. M. C. Foulkes, L. Mitas, R. J. Needs, and G. Rajagopal, Rev. Mod. Phys. **73**, 33 (2001).

[19] D. Varsano, S. Moroni, and G. Senatore, Europhys. Lett. **53**, 348 (2001).

[20] M. W. C. Dharma-wardana and F. Perrot, Phys. Rev. Lett. **90**, 136601 (2003).

[21] B. Tanatar and D. M. Ceperley, Phys. Rev. B **39**, 5005 (1989).

[22] M. Marchi, S. De Palo, S. Moroni, and G. Senatore, Phys. Rev. B **80**, 035103 (2009).

[23] C. Attaccalite, S. Moroni, P. Gori-Giorgi, and G. B. Bachelet, Phys. Rev. Lett. **88**, 256601 (2002).

[24] A. Camjayi, K. Haule, V. Dobrosavljevic, and G. Kotliar, Nat. Phys. **4**, 932 (2008).

[25] M. M. Radonjic, D. Tanaskovic, V. Dobrosavljevic, K. Haule, and G. Kotliar, Phys. Rev. B **85**, 085133 (2012).

[26] G. Fleury and X. Waintal, Phys. Rev. B **81**, 165117 (2010).

[27] D. Simonian, S. V. Kravchenko, M. P. Sarachik, and V. M. Pudalov, Phys. Rev. Lett. **79**, 2304 (1997).

[28] V. M. Pudalov, G. Brunthaler, A. Prinz, and G. Bauer, Pis'ma Zh. Eksp. Teor. Fiz. **65**, 887 (1997) [JETP Lett. **65**, 932 (1997)].

[29] H. Fukuyama, J. Phys. Soc. Jpn. **50**, 3407 (1981).

[30] B. L. Altshuler, A. G. Aronov, and A. Yu. Zyuzin, Pis'ma ZhETF **35**, 15 (1982) [JETP Lett. **35**, 16 (1982)].

[31] A. V. Chubukov and D. L. Maslov, Phys. Rev. B **68**, 155113 (2003).

[32] D. Belitz, T. R. Kirkpatrick, and T. Vojta, Phys. Rev. B **55**, 9452 (1997).

[33] V. M. Galitski, A. V. Chubukov, and S. Das Sarma, Phys. Rev. B **71**, 201302(R) (2005).

[34] J. Betouras, D. Efremov, and A. Chubukov, Phys. Rev. B **72**, 115112 (2005).

[35] A. V. Chubukov, D. L. Maslov, S. Gangadharaiah, and L. I. Glazman, Phys. Rev. Lett. **95**, 026402 (2005).

[36] G. Y. Chitov and A. J. Millis, Phys. Rev. Lett. **86**, 5337 (2001).

[37] N. N. Klimov, D. A. Knyazev, O. E. Omel'yanovskii, V. M. Pudalov, H. Kojima, and M. E. Gershenson, Phys. Rev. B **78**, 195308 (2008).

[38] A. Yu. Kuntsevich, N. N. Klimov, S. A. Tarasenko, N. S. Averkiev, V. M. Pudalov, H. Kojima, and M. E. Gershenson, Phys. Rev. B **75**, 195330 (2007).

[39] G. Zala, B. N. Narozhny, and I. L. Aleiner, Phys. Rev. B **64**, 214204 (2001); **65**, 020201 (2002).

[40] For high mobility S-MOS samples, in the temperature interval of our interest $\tau/\tau_v \ll T\tau < 1$, interaction correction $\Delta\chi^*$, Eq. (5), is not affected by the intervalley scattering time τ_v which is about $(10-15)\tau$ [38].

[41] V. M. Pudalov, M. E. Gershenson, H. Kojima, G. Brunthaler, A. Prinz, and G. Bauer, Phys. Rev. Lett. **91**, 126403 (2003).

[42] A. M. Finkelstein, Zh. Eksp. Teor. Fiz. **84**, 168 (1983) [Sov. Phys. JETP **57**, 97 (1983)].

[43] C. Castellani, C. Di Castro, P. A. Lee, M. Ma, S. Sorella, and E. Tabet, Phys. Rev. B **30**, 1596 (1984).

[44] C. Castellani, C. Di Castro, and P. A. Lee, Phys. Rev. B **57**, R9381 (1998).

[45] A. Punnoose and A. M. Finkel'stein, Science **310**, 289 (2005).

[46] V. Dobrosavljević, E. Abrahams, E. Miranda, and S. Chakravarty, Phys. Rev. Lett. **79**, 455 (1997).

[47] V. A. Khodel and V. R. Shaginyan, Pis'ma ZhETF **51**, 488 (1990) [JETP Lett. **51**, 553 (1990)].

[48] J. W. Clark, V. A. Khodel, and M. V. Zverev, Phys. Rev. B **71**, 012401 (2005).

[49] V. V. Borisov and M. V. Zverev, Pis'ma ZhETF **81**, 623 (2005) [JETP Lett. **81**, 503 (2005)].

[50] A. V. Andreev and A. Kamenev, Phys. Rev. Lett. **81**, 3199 (1998).

[51] A. A. Shashkin, Maryam Rahimi, S. Anissimova, S. V. Kravchenko, V. T. Dolgopolov, and T. M. Klapwijk, Phys. Rev. Lett. **91**, 046403 (2003).

[52] D. A. Knyazev, O. E. Omel'yanovskii, V. M. Pudalov, I. S. Burmistrov, Phys. Rev. Lett. **100**, 046405 (2008).

[53] S. Anissimova, S. V. Kravchenko, A. Punnoose, A. M. Finkel'stein, and T. M. Klapwijk, Nat. Phys. **3**, 707 (2007).

[54] A. Punnoose and A. M. Finkel'stein, Phys. Rev. Lett. **88**, 016802 (2001).

[55] A. Punnoose, A. M. Finkel'stein, A. Mokashi, and S. V. Kravchenko, Phys. Rev. B **82**, 201308 (2010).

[56] L. A. Morgun, A. Yu. Kuntsevich, and V. M. Pudalov, Phys. Rev. B **93**, 235145 (2016).

[57] V. M. Pudalov, L. A. Morgun, and A. Y. Kuntsevich, J. Supercond. Nov. Magn. **30**, 783 (2017).

[58] A. Yu. Kuntsevich, L. A. Morgun, and V. M. Pudalov, Phys. Rev. B **87**, 205406 (2013).

[59] N. Teneh, A. Yu. Kuntsevich, V. M. Pudalov, and M. Reznikov, Phys. Rev. Lett. **109**, 226403 (2012).

[60] O. Prus, Y. Yaish, M. Reznikov, U. Sivan, and V. Pudalov Phys. Rev. B **67**, 205407 (2003).

[61] A. A. Shashkin, S. Anissimova, M. R. Sakr, S. V. Kravchenko, V. T. Dolgopolov, and T. M. Klapwijk, Phys. Rev. Lett **96**, 036403 (2006).

[62] A. Shekhter and A. M. Finkel'stein, Proc. NAS **103**, 15765 (2006).

[63] A. Shekhter and A. M. Finkel'stein, Phys. Rev. B **74**, 205122 (2006).

[64] Y. V. Stadnik and O. P. Sushkov, Phys. Rev. B **88**, 125402 (2013).

[65] M. E. Gershenson, V. M. Pudalov, H. Kojima, N. Butch, E. M. Dizhur, G. Brunthaler, A. Prinz, and G. Bauer, Physica E **12**, 585 (2002).

[66] O. Prus, M. Reznikov, and U. Sivan, and V. M. Pudalov, Phys. Rev. Lett. **88**, 016801 (2001).

[67] I. M. Lifshitz and A. M. Kosevich, Zh. Eksp. Teor. Fiz. **33**, 88 (1958) [Sov. Phys. JETP **6**, 67 (1958)].

[68] A. Isihara, L. Smrcka, J. Phys. C: Solid State Phys. **19**, 6777 (1986).

[69] Yu. A. Bychkov, and L. P. Gor'kov, Zh. Exp. Teor. Fiz. **41**, 1592 (1962) [Sov. Phys.: JETP **14**, 1132 (1962)].

[70] V. M. Pudalov, M. E. Gershenson, and H. Kojima, Phys. Rev. B **90**, 075147 (2014).

[71] V. M. Pudalov and S. G. Semenchinskii, Pis'ma Zh. Exp. Teor. Fiz. **44**, 526 (1986) [JETP Lett. **44**, 677 (1986)].

[72] A. H. MacDonald, H. C. A. Oji, and K. L. Liu, Phys. Rev. B **34**, 2681 (1986).

[73] S. V. Kravchenko, D. A. Rinberg, S. G. Semenchinsky, and V. M. Pudalov, Phys. Rev. B **42**, 3741 (1990).

[74] V. M. Pudalov and M. E. Gershenson, J. Supercond. Novel Magn. **31**, 723 (2018).

[75] V. M. Pudalov, M. Gershenson, A. Yu. Kuntsevich, N. Teneh, and M. Reznikov, J. Magn. Magn. Mater. **459**, 265 (2018).

[76] M. Reznikov, A. Yu. Kuntsevich, N. Teneh, V. M. Pudalov, Pis'ma ZhETF **92**, 518 (2010) [JETP Lett. **92**, 470 (2010)].

[77] V. M. Pudalov, G. Brunthaler, A. Prinz, and G. Bauer, Physica B **249-251**, 697 (1998).

[78] S. A. Vitkalov, H. Zheng, K. M. Mertes, M. P. Sarachik, and T. M. Klapwijk, Phys. Rev. Lett. **85**, 2164 (2000).

[79] M. D'Iorio, V. M. Pudalov, and S. G. Semenchinsky, Phys. Rev. B **46**, 15992 (1992).

[80] V. M. Pudalov, M. D'Iorio, S. V. Kravchenko, and J. W. Campbell, Phys. Rev. Lett. **70**, 1866 (1993).

[81] M. D'Iorio, V. M. Pudalov, and S. G. Semenchinsky, Phys. Lett. A **150**, 422 (1990).

[82] V. M. Pudalov, M. D'Iorio, and J. W. Campbell, Surf. Sci. **305**, 107 (1994).

[83] S. V. Kravchenko, A. A. Shashkin, D. A. Bloore, and T. M. Klapwijk, Sol. State Commun. **116**, 495 (2000).

[84] V. M. Pudalov, J. de Phys. IV (France) **12**, 331 (2002).

[85] V. M. Pudalov, M. E. Gershenson, and H. Kojima, arXiv:cond-mat/0110160.

[86] V. M. Pudalov, G. Brunthaler, A. Prinz, and G. Bauer, Phys. Rev. Lett. **88**, 076401 (2002).

[87] Y. Zhang and S. Das Sarma, Phys. Rev. Lett. **96**, 196602 (2006).

[88] S. V. Kravchenko, Solid State Commun. **144**, 512 (2007).

[89] M. Reznikov and U. Sivan, arXiv:cond-mat/0410409

[90] M. M. Qazilbash, M. Brehm, B.-G. Chae, P.-C. Ho, G. O. Andreev, B.-J. Kim, S. J. Yun, A. V. Balatsky, M. B. Maple, F. Keilmann, H.-T. Kim, and D. N. Basov, Science **318**, 1750 (2007).

[91] Ya. A. Gerasimenko, S. V. Sanduleanu, V. A. Prudkoglyad, A. V. Kornilov, J. Yamada, J. S. Qualls, and V. M. Pudalov, Phys. Rev. B **89**, 054518 (2014).

[92] A. V. Kornilov, V. M. Pudalov, Y. Kitaoka, K. Ishida, G.-q. Zheng, T. Mito, and J. S. Qualls, Phys. Rev. B **69**, 224404 (2004).

[93] V. M. Pudalov, J. Supercond. Nov. Magn. **30**, 69 (2017).
[94] I. S. Burmistrov and N. M. Chtchelkatchev, Phys. Rev. B **77**, 195319 (2008).
[95] I. S. Burmistrov, in *Strongly Correlated Electrons in Two Dimensions*, edited by S. V. Kravchenko (Pan Stanford Publishing Pte. Ltd., Singapore, 2017), pp. 65–116.
[96] V. M. Pudalov, S. G. Semenchinskii, and V. S. Edel'man, Pis'ma ZhETF **39**, 474 (1984) [JETP Lett. **39**, 576 (1984)].
[97] G. W. Martin, D. L. Maslov, and M. Yu. Reizer, Phys. Rev. B **68**, 241309(R) (2003).
[98] Y. Adamov, I. V. Gornyi, and A. D. Mirlin, Phys. Rev. B **73**, 045426 (2006).